Control Engineering Practice 63 (2017) 91–103

Contents lists available at ScienceDirect

Control Engineering Practice

journal homepage: www.elsevier.com/locate/conengprac

Longitudinal tunnel ventilation control. Part 1: Modelling and dynamic feedforward control

Nikolaus Euler-Rolle[a,*], Martin Fuhrmann[a], Markus Reinwald[b], Stefan Jakubek[a]

[a] TU Wien, Institute of Mechanics and Mechatronics, Getreidemarkt 9/325/A5, 1060 Vienna, Austria
[b] ASFINAG Bau Management GmbH, Fuchsenfeldweg 71, 8074 Graz-Raaba, Austria

ARTICLE INFO

Keywords:
Tunnel ventilation
Jet fan control
Dynamic feedforward control
Two-degrees-of-freedom control
Over-actuated system

ABSTRACT

Road tunnels exceeding a certain minimum length are equipped with a ventilation system. In case of a fire it is used to achieve a predefined air flow velocity in the tunnel by adequately controlling the installed jet fans in order to ensure sufficient visibility for persons to safely follow the escape routes. As the dynamics of the air flow in road tunnels strongly depend on the tunnel length, short tunnels with longitudinal ventilation systems pose a challenging control task. In this paper, non-linear dynamic feedforward control is proposed for longitudinal ventilation control in case of an emergency. For this purpose, an analytical non-linear zero-dimensional model of the air flow is feedback linearised. Due to its special properties, which are presented and analysed, two different versions of feedforward control are proposed: One is focused on performance, the other on robustness. Finally, the beneficial behaviour of the presented two-degrees-of-freedom control approach is demonstrated by its application to an Austrian motorway tunnel.

1. Introduction

New constructions or refurbishments of road tunnels impose increasingly tight safety requirements on the electrotechnical tunnel equipment such as the ventilation system, as well as on its operation. Particularly in the event of an incident with fire and smoke spreading in the tunnel, adequate safety measures have to be taken without delay to protect life and health of the tunnel users. The main goal is to guarantee a minimum amount of time for persons in the tunnel to safely follow the escape routes with sufficient visibility available. For this purpose, tunnels exceeding a certain minimum length are equipped with ventilation systems. There exist several, very different approaches to ventilation concepts (Sturm, Beyer, & Rafiei, 2015; PIARC, 2011; Bendelius, 1996). In this paper, longitudinal ventilation is considered in case of an emergency, where jet fans are used to induce fresh air into the tunnel through one portal and exhaust the smoke through the other. However, since the spread of smoke in the tunnel can not be measured in tunnels with longitudinal ventilation, it is assumed that a safe condition is achieved by maintaining an average air flow velocity in the tunnel, which is high enough to convey smoke out of the tunnel, but not too high to save the naturally occurring smoke stratification from being destroyed. Thus, appropriate and accurate jet fan control is critical to achieve a satisfactory control performance and provide the opportunity for persons to escape safely, respectively. In this context, control is especially challenging for short tunnels due to their low inertia and the resulting highly dynamic behaviour. In shorter tunnels, the overall air mass located within the tunnel is lower, which leads to a more imminent effect of any momentum source (from jet fans or disturbances) on the rate of change of the air flow velocity.

In combination with tight trajectory tracking requirements, actuator saturation and the need to avoid undesired overshoot of the air flow velocity, a non-linear control scheme should beneficially be used to control the jet fans taking into account non-linearities of the jet fans as well as of the non-stationary Bernoulli equation as the tunnel air flow model. Especially as there are several disturbance influences such as vehicles in the tunnel, buoyancy of hot gases, wind load onto the portals or meteorological pressure differences influencing the flow velocity, an appropriate reference tracking as well as sufficiently fast disturbance rejection are required.

Usually, tunnel ventilation systems are controlled by standard linear feedback controllers such as PI or PID controllers. However, these conventional control schemes reach their limits of applicability as soon as non-linear effects become increasingly dominant. On the one hand, a tradeoff between reference tracking performance and disturbance rejection capability has to be made in the controller tuning. On the other hand, as the non-linear effects grow stronger and the system state lies further away from the plant linearisation point, the closed

* Corresponding author.
E-mail addresses: nikolaus.euler-rolle@tuwien.ac.at (N. Euler-Rolle), martin.fuhrmann@tuwien.ac.at (M. Fuhrmann), markus.reinwald@asfinag.at (M. Reinwald), stefan.jakubek@tuwien.ac.at (S. Jakubek).

http://dx.doi.org/10.1016/j.conengprac.2017.03.017
Received 21 September 2016; Received in revised form 27 March 2017; Accepted 29 March 2017
Available online 20 April 2017

Nomenclature

List of variables

$A_{JV,i}$	cross sectional area of jet fan i
A_{Tunnel}	cross sectional area of the tunnel
c	abbreviation defined in (34).
$d(\boldsymbol{x})$	thrust distribution function/algorithm
D_{hydr}	hydraulic diameter of the tunnel
$\boldsymbol{e}$	model error vector in the parameter optimisation
$\boldsymbol{f}$	system dynamics of the state space model
$\boldsymbol{g}_i$	affine input function of input i of the state space model
h	output function of the state space model
$k_{e,i}$	installation factor of jet fan i
k_{Fric}	overall friction coefficient
$k_{JV,i}$	thrust coefficient of jet fan i
L	tunnel length
$\mathcal{L}$	cost function in the parameter optimisation
$L_f h$	Lie derivative of h along vector field $\boldsymbol{f}$
n	state space system dimension
n_{JV}	number of installed jet fans
n_{on}	number of jet fans fully switched on
n_s	dimension of model error vector $\boldsymbol{e}$
Δp	equivalent pressure difference
r	relative degree
$\boldsymbol{R}$	weighting matrix in the parameter optimisation
$R(\boldsymbol{x}^*, n_{on})$	abbreviation defined in (38).
$\mathcal{T}$	diffeomorphism from $\boldsymbol{x}$ to $\boldsymbol{z}$
u	air flow velocity
u_m	air flow velocity measurement
u^*	feasible air flow velocity
u_m^*	feasible air flow velocity considering measurement dynamics
v	virtual input to the external dynamics
$v_{JVmax,i}$	maximum average outlet velocity of jet fan i
w	air flow velocity reference
$\boldsymbol{x}$	state vector
$\boldsymbol{x}^*$	required state trajectory associated with w
${}^{+}x_2^*$	req. trajectory of x_2 associated with w (solution 1)
${}^{-}x_2^*$	req. trajectory of x_2 associated with w (solution 2)
y	output of the state space system
z	state vector of the transformed system
$\boldsymbol{\Delta}$	disturbance input of the state space system
λ	wall friction coefficient
ω_i	dimensionless rotational speed of jet fan i
ω_{dmd}	dimensionless rotational speed reference
ω_{dmd}^*	dimensionless rot. speed ref. from feedforward control
${}^{+}\omega_{dmd}^*$	rot. speed ref. from feedforward control (solution 1)
${}^{-}\omega_{dmd}^*$	rot. speed ref. from feedforward control (solution 2)
ω_v	virtual rotational speed of a single substitute jet fan
ω_n	undamped natural angular frequency of the ref. generation
$\boldsymbol{\Psi}$	weighting matrix in the parameter optimisation
ρ	air density within the tunnel
$\boldsymbol{\theta}_0$	initial parameter vector in the parameter optimisation
$\boldsymbol{\Delta\theta}$	parameter vector deviation from $\boldsymbol{\theta}_0$
$\tilde{\Sigma}_{ol}$	open loop plant model
$\tilde{\Sigma}_{ol}^{-1}$	inverse open loop plant model
Σ_m	measurement dynamics
$\tilde{\Sigma}_m$	model of the measurement dynamics
Σ_C	feedback controller
σ	step signal applied in the ref. generation
τ_{JV}	time constant of the jet fan thrust buildup
τ_m	time constant of the measurement dynamics
ζ_E	factor describing influx losses in the friction coefficient
ζ	damping ratio used in the ref. generation

loop performance decreases. When non-linear feedforward control is used as an extension of standard feedback control, a feedback controller tuning specific to disturbance rejection can be applied. Thus, an improved closed loop performance is achieved across the whole operating range.

In advanced and non-linear control schemes, the application of feedforward control is state of the art. Usually, a dynamic feedforward control law is obtained by some kind of model inversion. Whereas most applications are based on a design using feedback linearisation (Hagenmeyer & Delaleau, 2003), system inversion still remains a challenging task. For that reason, a profound analysis and knowledge of the non-linear system under consideration is required. Applications of feedforward control can be found in a variety of fields, such as for example the actuation of hydraulic automotive clutches (Horn, Bamberger, Michau, & Pindl, 2003), temperature control of industrial processes (Malchow & Sawodny, 2012) or the gas supply of fuel cells (Danzer, Wilhelm, Aschemann, & Hofer, 2008).

In the literature, advanced control methodologies for tunnel ventilation have been mainly proposed for normal tunnel operation only. In contrast to emergency ventilation, the main goal in normal operation is to comply with restrictions imposed on the opacity, as well as on the concentrations of air pollutants within the tunnel such as NO_x or CO. Several control strategies have been applied in combination with different model configurations. Hrbcek, Spalek, and Šimák (2010) combine model predictive jet fan control with autoregressive moving-average models describing the pollution concentrations. Kurka, Ferkl, Porízek, and Jul (2005) as well as Ferkl and Meinsma (2007) use a model, which is split into submodels with different one-dimensional spatial discretisations to simulate traffic, ventilation and pollutant concentrations. The simulation is performed on a car by car basis and the effect of ventilation is considered by the steady-state Bernoulli equation. Tan et al. (2012) performed 3D CFD simulations of pollutant levels and extracted step response features from the data to apply dynamic matrix control. Also fuzzy models have been applied several times for prediction and simulation of pollutant concentrations (Chen, Lai, & Lin, 1998). Bogdan, Birgmajer, and Kovačić (2008) developed a static feedforward control for the number of necessary jet fans and combined it with fuzzy control to meet the air quality limits. Based on the prediction of the required air flow (depending on traffic and weather conditions), the number of currently required jet fans is found from the steady-state Bernoulli equation based on an estimated tunnel air speed necessary to supply the required air mass flow. In contrast to the proposed model-based dynamic feedforward control, Bogdan et al. (2008) consider the pollutant levels only and no dynamic behaviour of the air flow velocity is considered. In normal operation, in addition to the achievement of appropriate pollutant levels, also the minimisation of power consumption has been demonstrated by fuzzy predictive control (Karakas, 2003) or genetic algorithms in combination with fuzzy control (Chu et al., 2008). However, all these contributions deal with normal tunnel operation only and do not consider the dynamic behaviour of the air flow velocity.

Emergency ventilation has been treated by Nakahori, Mitani, and Vardy (2010) in a simulation study using an encompassing automatic control system for long two-way road tunnels with longitudinal ventilation. However, the focus is rather on overall control system considerations than on the specific feedback and feedforward control design.

In the present paper, model-based non-linear dynamic feedforward control is applied to the longitudinal tunnel ventilation to enhance standard feedback control and improve the closed-loop behaviour. The

generation of feedforward control is based on differential geometric properties of the dynamic air flow model and has also been tested in a tunnel with and without an actual fire. The combination of feedback Σ_C and feedforward control $\widetilde{\Sigma}_{ol}^{-1}$ in a two-degrees-of-freedom control scheme is depicted in Fig. 1. It consists of the plant, a feedback controller Σ_C, an air flow velocity measurement device Σ_m as well as its model $\widetilde{\Sigma}_m$ and the feedforward control $\widetilde{\Sigma}_{ol}^{-1}$, which is based on the open loop plant model $\widetilde{\Sigma}_{ol}$. Signals computed by the feedforward control are asterisked. Applying such a control scheme allows for requirements on the reference trajectory tracking to be separated from requirements on robustness and disturbance attenuation. Thus, the design of the feedforward part and the feedback part are independent of each other (Horowitz, 1963). In the combined control scheme, based on the reference trajectory w of the flow velocity u (controlled variable) the feedforward part generates a control signal ω_{dmd}^* denoting the normalised demanded rotational speed of the jet fans. This feedforward control signal is added to the control signal of the correcting feedback control Σ_C. Additionally, a feasible flow velocity trajectory u^*, which will be achieved by applying the feedforward control signal ω_{dmd}^* to the jet fans, is calculated. As the feedback control Σ_C has only the measured air flow velocity u_m available, which is influenced by the measurement dynamics Σ_m, the reference u_m^*, which is passed to the control loop, has to consider a model of the measurement dynamics $\widetilde{\Sigma}_m$. These dynamics can also incorporate a time delay. If parameter uncertainties or model errors occur in the open-loop plant model $\widetilde{\Sigma}_{ol}$ and in the feedforward control $\widetilde{\Sigma}_{ol}^{-1}$, respectively, the feedback part will still track the reference trajectory, try to compensate for the inaccuracies and improve control performance. Due to the structure of the overall control scheme, also a higher time delay in the measurement dynamics does not cause any undesired delay in the closed-loop system response.

As there is normally more than one jet fan installed in the tunnel, multiple actuators are available to introduce momentum into the air flow. Thus, the plant is over-actuated, because several control signals influence one single controlled variable. However, as all the actuators are jet fans and have the same principle of operation, a distribution algorithm can be used in the dynamic feedforward control to achieve the desired overall momentum intake with different possible actuator configurations.

Before being able to apply feedback control, relevant parameters of the non-stationary Bernoulli equation representing the analytic zero-dimensional model of the tunnel air flow have to be identified from data and validated. This is achieved by performing open-loop experiments with suitable jet fan control signals. The resulting measured air flow velocity trajectory is then used to adjust relevant parameters by optimisation using the output error method (Ljung, 1999).

The proposed approach for the generation of the feedforward control law $\widetilde{\Sigma}_{ol}^{-1}$ is based on feedback linearisation (Isidori, 1995; Slotine & Li, 1991) as a non-linear system transformation. Feedback linearisation is applied to the air flow model, and the resulting non-linear relation describing the input is used as model inverse for feedforward control of the rotational speeds of the jet fans. However, when applying this relation, controllability issues in combination with a bifurcation characteristic caused by the absolute values in the Bernoulli equation occasionally lead to implausible control signals. Thus, for a flawlessly robust operation in different conditions, these issues require a modified evaluation of the feedforward control. Instead of the original expression resulting from feedback linearisation, a modified robustness-oriented feedforward control is based on the state transformation for trajectory evaluation in combination with control loops to actuate the individual jet fans. The advantage of significantly improved robustness is achieved at the expense of a slight performance reduction of the feedforward control part.

This paper is the first of two papers dealing with non-linear tunnel ventilation control. The second part (Fuhrmann, Euler-Rolle, Killian, Reinwald, & Jakubek, 2017) focuses on non-linear disturbance observation of external influences and compensation, which is achieved by applying a specially structured non-linear observer, showing its stability as well as its application for disturbance compensation. Meanwhile, in this paper in Section 2 the non-linear model of tunnel air flow and its assumptions are presented. Section 3 gives a short introduction into model-based feedforward control in general. The design of the tunnel ventilation feedforward control, including an analysis of controllability and details about trajectory planning are given in Section 4. Finally, in Section 5 the application of two-degrees-of-freedom control in course of a fire test demonstrates the control performance in an experiment. The paper is concluded by an outlook in Section 6.

2. Non-linear model of tunnel air flow

To model the air flow in road tunnels equipped with longitudinal ventilation, approaches with different foci can be pursued. A flow model needs not to be focussed solely on an event with fire and smoke, but in many cases treats the normal tunnel operation, where emission concentration control is the main objective. Thus, also the concepts of control usually focus either on one or the other case, and are specifically designed for their intended application. A brief introduction into modelling is given by Sturm, Bacher, Schmölzer, and Beyer (2010), where an overview of possible methods for the design and validation of tunnel models is given.

Since in emergency ventilation control the average flow velocity is considered only and spread of smoke or heat release are not treated directly, the application of a zero-dimensional model is sufficient. In consequence, the tunnel is considered as concentrated system without spatial extension as the air within the tunnel is assumed to be incompressible. In this modelling approach various relevant sources and losses of momentum can be taken into account. However, all quantities must represent mean values, either over the tunnel cross section (such as e. g. the flow velocity) or the length of the tunnel (such as e. g. the air density).

In Fig. 2 a schematic overview of the air flow model and the individual sources of momentum in form of equivalent pressure differences $\Delta p_j(t)$ is given. The controlled input $\omega_{dmd,i}(t)$ into the model is the demanded rotational speed of jet fan i described below, and the output is the air flow velocity $u(t)$. The dynamic behaviour of the flow velocity $u(t)$ is described by the incompressible non-stationary Bernoulli equation yielding a non-linear ordinary differential equation of first order

$$\frac{du(t)}{dt} = \sum_{i=1}^{n_{JV}} k_{JV,i} v_{JVmax,i}^2 |\omega_i(t)| \omega_i(t) \left(1 - \frac{u(t)}{\omega_i(t) v_{JVmax,i}}\right) - k_{Fric} u(t) |u(t)| + \sum_j \frac{\Delta p_j(t)}{\rho L}, \quad j \in \{\text{Wind, MV, Stack, Meteo}\}. \tag{1}$$

The first sum in (1) describes the effect of the n_{JV} jet fans on the flow velocity. Each fan indexed by i is characterised by its maximum average outlet velocity $v_{JVmax,i}$ and by the factor

$$k_{JV,i} = \frac{1}{L} \frac{A_{JV,i}}{A_{Tunnel}} k_{e,i} \tag{2}$$

with L describing the tunnel length, A_{JV} the cross sectional area of the ventilator, A_{Tunnel} the cross sectional area of the tunnel and $k_{e,i}$ a correction factor considering the installation situation of the ventilator (Cory, 2005). The dimensionless rotational speed $\omega_i(t)$ of jet fan i

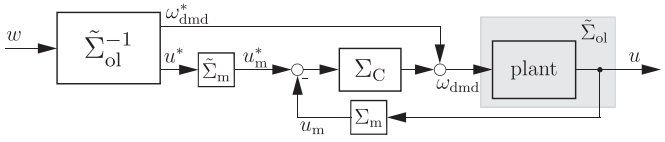

Fig. 1. Block diagram of the two-degrees-of-freedom control scheme.

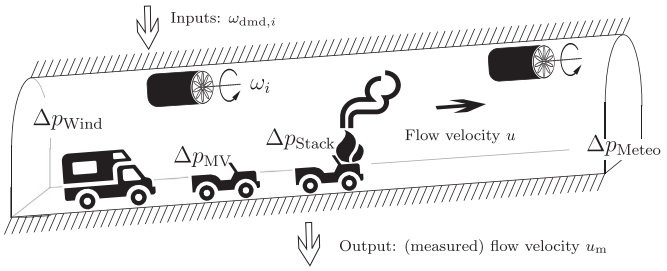

Fig. 2. Schematic overview of the air flow model showing the inputs, the output and the individual sources and losses of momentum.

represents the ratio of the current to the maximum rotational speed. All jet fans can operate in both directions with the same parameters. Thus, if a frequency converter is available, $\omega_{\mathrm{dmd},i}(t)$ can take any value between -1 and 1, otherwise only zero and ± 1 exactly. For the dimensionless rotational speed $\omega_i(t) \in [-1; 1]$ holds in either case. By convention, the sign of the rotational speeds $\omega_i(t)$ and $\omega_{\mathrm{dmd},i}(t)$ of the jet fans is positive, if they generate a momentum in the positive flow direction.

The second term in (1) characterises the wall friction as well as flow losses decelerating the air flow. The factor

$$k_{\mathrm{Fric}} = \frac{1}{2L}\left[\frac{\lambda L}{D_{\mathrm{hydr}}} + \zeta_{\mathrm{E}} + 1\right] \tag{3}$$

incorporates the hydraulic diameter D_{hydr} of the tunnel, the wall friction coefficient λ, which considers obstructing installations in the tunnel, and the factor ζ_{E} describing influx losses. Any additional influences such as the stack effect, vehicle movement, buoyancy, wind load on the portal or meteorological pressure differences can be included in the last sum term in (1) in form of equivalent pressure differences $\Delta p_j(t)$. Therein, the air density in the tunnel is denoted by ρ. A density change due to pressure differences is not considered, whereas the dependency of the density on the temperature in the tunnel can be included into the model. From the zero-dimensional approach, it follows that the density of the air in the tunnel is only a spatial mean value. In turn, the mean temperature has to be used to determine the current air density. In general, temperature differences between inside and outside of the tunnel can be incorporated into the model by buoyancy, provided a longitudinal road gradient unequal to zero applies. For the case of a fire there exist approximations how the average temperature i. e. air density in the tunnel can be determined (see the Austrian standard RVS, 2014). Although all the individual disturbances $\Delta p_j(t)$, where j represents the index of different influences, could be included into the feedforward control easily, they are assumed to be zero in the feedforward control, because they are usually unknown. In the second paper (Fuhrmann et al., 2017) the disturbance observation is shown.

To represent the dynamic relation between the control signals $\omega_{\mathrm{dmd},i}(t)$ of the jet ventilators and the current dimensionless rotational speeds $\omega_i(t)$, which determine the current thrust, a first-order low-pass behaviour with appropriate time constant τ_{JV} is assumed

$$\frac{\mathrm{d}\omega_i(t)}{\mathrm{d}t} = \frac{1}{\tau_{\mathrm{JV},i}}(\omega_{\mathrm{dmd},i}(t) - \omega_i(t)). \tag{4}$$

It takes into account the necessary acceleration of the fanwheel as well as the thrust buildup.

The model of the measurement dynamics $\widetilde{\Sigma}_{\mathrm{m}}$, which is applied as shown in Fig. 1, is again assumed as first-order low-pass filter with time constant τ_{m}

$$\frac{\mathrm{d}u_{\mathrm{m}}(t)}{\mathrm{d}t} = \frac{1}{\tau_{\mathrm{m}}}(u(t) - u_{\mathrm{m}}(t)). \tag{5}$$

However, this relation is not used in the feedforward control design directly. Thus, for further considerations (1) and (4) are formulated as a non-linear state space system of the form

$$\frac{\mathrm{d}\boldsymbol{x}(t)}{\mathrm{d}t} = \boldsymbol{f}(\boldsymbol{x}(t)) + \sum_{i=1}^{n_{\mathrm{JV}}} \boldsymbol{g}_i(\boldsymbol{x}(t))\omega_{\mathrm{dmd},i}(t) + \boldsymbol{\Delta}(t) \tag{6a}$$

$$y(t) = h(\boldsymbol{x}(t)) = x_1(t) \tag{6b}$$

with state vector $\boldsymbol{x}(t) \in \mathbb{R}^{(n_{\mathrm{JV}}+1)}$

$$\boldsymbol{x}(t) = [u(t), \omega_1(t), \ldots, \omega_{n_{\mathrm{JV}}}(t)]^{\mathrm{T}} \tag{7}$$

scalar inputs $\omega_{\mathrm{dmd},i}(t)$, scalar output $y(t)$, smooth vector fields $\boldsymbol{f}\colon \mathbb{R}^{(n_{\mathrm{JV}}+1)} \to \mathbb{R}^{(n_{\mathrm{JV}}+1)}$ and $\boldsymbol{g}_i\colon \mathbb{R}^{(n_{\mathrm{JV}}+1)} \to \mathbb{R}^{(n_{\mathrm{JV}}+1)}$ as well as a smooth function $h\colon \mathbb{R}^{(n_{\mathrm{JV}}+1)} \to \mathbb{R}$. The term $\boldsymbol{\Delta}(t) \in \mathbb{R}^{(n_{\mathrm{JV}}+1)}$ contains any external disturbances acting on the flow velocity.

Finally, the first row of (6a) reads

$$\dot{x}_1(t) = \sum_{i=1}^{n_{\mathrm{JV}}} k_{\mathrm{JV},i} v_{\mathrm{JVmax},i}^2 |x_{i+1}(t)| \left(x_{i+1}(t) - \frac{x_1(t)}{v_{\mathrm{JVmax},i}}\right) - k_{\mathrm{Fric}} x_1(t)|x_1(t)| + \sum_j \frac{\Delta p_j(t)}{\rho L} \quad j \in \{\mathrm{Wind}, \mathrm{MV}, \mathrm{Stack}, \mathrm{Meteo}\}. \tag{8}$$

and the remaining n_{JV} rows for $i = \{2, \ldots, n_{\mathrm{JV}} + 1\} \in \mathbb{N}$ as

$$\dot{x}_i(t) = -\frac{1}{\tau_{\mathrm{JV},i-1}} x_i(t) + \frac{1}{\tau_{\mathrm{JV},i-1}} \omega_{\mathrm{dmd},i-1}(t). \tag{9}$$

The system output is the flow velocity in the tunnel, thus for (6b)

$$y(t) = h(t) = x_1(t) \tag{10}$$

holds.

The influence of measurement dynamics is not considered in the design of the feedforward control directly. However, its consideration is necessary in the overall two-degrees-of-freedom control scheme as shown in Fig. 1. This fact especially applies to the design of the feedback controller. Otherwise, a dead time or any other delays induced by the flow velocity sensor could deteriorate the closed-loop performance.

For the sake of clarity, time dependencies are omitted in the subsequent sections.

3. Model-based feedforward control

The generation of a dynamic feedforward control law from the non-linear plant model is achieved by applying feedback linearisation, which is also referred to as exact linearisation (Isidori, 1995; Khalil, 2002; Slotine & Li, 1991). By feedback linearisation a system transformation of a non-linear system into an equivalent linear system through a change of variables and a suitable control input is performed such that it renders a linear input-output map between a new (virtual) input v and the output. Initially assume that only one jet fan exists ($n_{\mathrm{JV}} = 1$), so that a single input, single output system with state dimension $n = n_{\mathrm{JV}} + 1 = 2$ can be considered. In addition, any disturbances Δp_j are neglected.

To obtain the required transformation, the system output y, which represents the flow velocity in case of the tunnel model, is differentiated repeatedly with respect to time along a solution trajectory of the state space system (6) until the control signal ω_{dmd} appears explicitly in the derivative. The first derivative of the output y yields

$$\dot{y} = \frac{\partial h(\boldsymbol{x})}{\partial \boldsymbol{x}} \frac{\mathrm{d}\boldsymbol{x}}{\mathrm{d}t} \tag{11a}$$

$$= \frac{\partial h(\boldsymbol{x})}{\partial \boldsymbol{x}} (\boldsymbol{f}(\boldsymbol{x}) + \boldsymbol{g}(\boldsymbol{x})\omega_{\mathrm{dmd}}) \tag{11b}$$

$$= \mathrm{L}_f h(\boldsymbol{x}) + \mathrm{L}_g h(\boldsymbol{x})\omega_{\mathrm{dmd}} \tag{11c}$$

The expressions $\mathrm{L}_f h(\boldsymbol{x}) \in \mathbb{R}$ and $\mathrm{L}_g h(\boldsymbol{x}) \in \mathbb{R}$ in (11c) are the Lie derivatives (Slotine & Li, 1991) of the scalar function $h(\boldsymbol{x})$ along the vector fields $\boldsymbol{f}(\boldsymbol{x})$ and $\boldsymbol{g}(\boldsymbol{x})$, respectively. The Lie derivative

$L_f^k h(\boldsymbol{x})$, $k \in \mathbb{N}$ is defined recursively

$$L_f^k h(\boldsymbol{x}) = L_f(L_f^{k-1} h(\boldsymbol{x})), \tag{12a}$$

$$L_f^0 h(\boldsymbol{x}) = h(\boldsymbol{x}). \tag{12b}$$

The relative degree r of a system (6) is defined as the number of differentiations of the output y which have to be applied before the input ω_{dmd} appears in the resulting equation for the first time explicitly. Thus, by using Lie derivatives, the relative degree r at $\bar{\boldsymbol{x}}$ is determined by

$$L_g L_f^i h(\boldsymbol{x}) = 0, \quad i = 0, \ldots, r-2, \quad \forall\ \boldsymbol{x} \text{ in a neighbourhood of } \bar{\boldsymbol{x}} \tag{13a}$$

$$L_g L_f^{r-1} h(\bar{\boldsymbol{x}}) \neq 0. \tag{13b}$$

This leads to the following $r+1$ relations

$$y = h(\boldsymbol{x}) \tag{14a}$$

$$\dot{y} = L_f h(\boldsymbol{x}) \tag{14b}$$

$$\vdots$$

$$y^{(r-1)} = L_f^{r-1} h(\boldsymbol{x}) \tag{14c}$$

$$y^{(r)} = L_f^r h(\boldsymbol{x}) + L_g L_f^{r-1} h(\boldsymbol{x}) \omega_{\text{dmd}}. \tag{14d}$$

Particularly interesting is the case, if the relative degree r equals the system order n. Then, the system is said to have *full relative degree* and a differentially flat system is present. However, in general a relative degree less than the system dimension might appear.

To determine the relative degree of the tunnel ventilation, the Lie derivatives (13a) and (13b) are considered. The system structure under consideration is given by (6) with $\boldsymbol{\Delta} = \boldsymbol{0}$. This relation contains differential Eqs. (8) and (9). Evaluating (13a) for i=0 yields

$$L_g h(\boldsymbol{x}) = 0. \tag{15}$$

The result (15) reveals the relative degree r to be bigger than one. From

$$L_g L_f h(\boldsymbol{x}) = \operatorname{sign}(x_2) \frac{k_{\text{JV}}\, v_{\text{JVmax}}^2}{\tau_{\text{JV}}} \left(2x_2 - \frac{x_1}{v_{\text{JVmax}}} \right) \tag{16}$$

being unequal to zero, the relative degree r is found to be

$$r = 2. \tag{17}$$

The determined relative degree (17) holds under the assumption that only one jet fan exists. Thus, the tunnel ventilation with one jet fan has full relative degree.

If eventually a virtual input v is chosen to be

$$v \overset{!}{=} y^{(r)} = L_f^r h(\boldsymbol{x}) + L_g L_f^{r-1} h(\boldsymbol{x}) \omega_{\text{dmd}} \tag{18}$$

and a diffeomorphism $\mathcal{T}(\boldsymbol{x})$ is given by transformation into new coordinates $z \in \mathbb{R}^n$ according to

$$\boldsymbol{z} = \begin{bmatrix} z_1 \\ z_2 \\ \vdots \\ z_n \end{bmatrix} = \begin{bmatrix} y \\ \dot{y} \\ \vdots \\ y^{(n-1)} \end{bmatrix} = \mathcal{T}(\boldsymbol{x}), \tag{19}$$

then the original system (6) is transformed into a linear chain of r integrators called external dynamics

$$\begin{bmatrix} \dot{z}_1 \\ \dot{z}_2 \\ \vdots \\ \dot{z}_{n-1} \\ \dot{z}_n \end{bmatrix} = \begin{bmatrix} 0 & 1 & 0 & \cdots & 0 \\ 0 & 0 & 1 & \cdots & 0 \\ \vdots & \vdots & \vdots & \ddots & \vdots \\ 0 & 0 & 0 & \cdots & 1 \\ 0 & 0 & 0 & \cdots & 0 \end{bmatrix} \begin{bmatrix} z_1 \\ z_2 \\ \vdots \\ z_{n-1} \\ z_n \end{bmatrix} + \begin{bmatrix} 0 \\ 0 \\ \vdots \\ 0 \\ 1 \end{bmatrix} v \tag{20a}$$

$$y = z_1, \tag{20b}$$

which is driven by the virtual input v. In general, $\mathcal{T}: M \to N$ is a diffeomorphism if it is bijective and continuously differentiable with its inverse.

The combination of the linear external dynamics (20a), (20b) and the non-linear relation

$$\omega_{\text{dmd}} = \frac{v - L_f^r h(\boldsymbol{x})}{L_g L_f^{r-1} h(\boldsymbol{x})}, \tag{21}$$

resulting from (18) and (14d) yields exactly the same input output behaviour between ω_{dmd} and y as the original system (6). For the tunnel ventilation with relative degree r=2, based on the first order Lie derivative

$$L_f h(\boldsymbol{x}) = \sum_{i=1}^{n_{\text{JV}}} k_{\text{JV},i} v_{\text{JVmax},i}^2 |x_{i+1}| \left(x_{i+1} - \frac{x_1}{v_{\text{JVmax},i}} \right) - k_{\text{Fric}} x_1 |x_1|, \tag{22}$$

the second order derivative $L_f^2 h(\boldsymbol{x})$ in (21) yields

$$\begin{aligned} L_f^2 h(\boldsymbol{x}) = 2k_{\text{Fric}}^2 x_1^3 + \sum_{i=1}^{n_{\text{JV}}} \Bigg\{ & k_{\text{JV},i} v_{\text{JVmax},i} \Bigg[x_{i+1} k_{\text{Fric}} |u| (2|x_{i+1}| v_{\text{JVmax},i} + 3x_1) \\ & + \frac{|x_{i+1}|}{\tau_i} (2x_{i+1} v_{\text{JVmax},i} + x_1) \Bigg] \\ & - \sum_{j=1}^{n_{\text{JV}}} k_{\text{JV},i} k_{\text{JV},j} v_{\text{JVmax},i} v_{\text{JVmax},j}^2 |x_{i+1}| \|x_{j+1}| \left(x_{j+1} - \frac{x_1}{v_{\text{JVmax},j}} \right) \Bigg\}. \end{aligned} \tag{23}$$

Finally, the special system structure provides the opportunity to apply beneficial non-linear control approaches such as flatness-based dynamic feedforward control to the original system. For differentially flat systems (Fliess, Lévine, Martin, & Rouchon, 1995), the required feedforward control signal ω_{dmd}^* can be found directly from the reference trajectory w and the feedback linearised system (Hagenmeyer & Delaleau, 2003). As a differential geometric approach is used, also the derivatives of the reference trajectory up to order r are considered. The trajectory planning for the tunnel ventilation control will be presented in Section 4.5.

By replacing the actual output y in the inverse transformation $\mathcal{T}^{-1}(z)$ of (19) by the reference trajectory w and its derivatives, the required state trajectories $\boldsymbol{x}^* \in \mathbb{R}^n$, which have to be induced by the feedforward control signal, are found from the inverse transformation incorporating the diffeomorphism $\mathcal{T}$

$$\boldsymbol{x}^*(w, \dot{w}, \ldots, w^{(r-1)}) = \mathcal{T}^{-1} \left(\begin{bmatrix} w \\ \dot{w} \\ \vdots \\ w^{(r-1)} \end{bmatrix} \right). \tag{24}$$

With knowledge of $\boldsymbol{x}^*$ and the requirement $v = y^{(r)} \overset{!}{=} w^{(r)}$, (21) is then used to evaluate the required control signal ω_{dmd}^* from

$$\omega_{\text{dmd}}^* = \frac{w^{(r)} - L_f^r h(\boldsymbol{x}^*)}{L_g L_f^{r-1} h(\boldsymbol{x}^*)}. \tag{25}$$

For the tunnel ventilation (r=2), (25) is evaluated using the Lie derivatives (23) and (16) as well as the second derivative $\ddot{w}$ of the time dependent reference trajectory w. The state transformation $\mathcal{T}(\boldsymbol{x})$ and inverse transformation $\mathcal{T}^{-1}(z)$ will be given and analysed in Section 4.3. Comparing (25) to (21) reveals that (25) is based upon the reference trajectory w only. This property is specific to feedforward control laws. In contrast, (21) can be interpreted as a state dependent relation, which transforms the virtual control signal v to the physical control signal ω_{dmd}, where the current system state $\boldsymbol{x}$ is used.

If the plant model were exact with no parameter uncertainties or disturbances acting on the plant, the dynamic feedforward control law (25) would drive the system such that it exactly fulfils $v = w^{(r)}$, thus $y \equiv w$ holds along the whole trajectory. Disturbance attenuation is achieved by the feedback part in the two-degrees-of-freedom control scheme (Fig. 1). Alternatively, by using an appropriate observation or estimation of the disturbance, the disturbance could already be taken

into account by the feedforward control. This approach is pursued in the second paper (Fuhrmann et al., 2017) on non-linear tunnel ventilation control treating disturbance observation and compensation in detail with the proposition of a specially structured non-linear pressure drop observer.

Usually, in tunnels there is more than one jet fan available for the control of the air flow velocity. Thus, the system description (6a) incorporates n_{JV} control signals $\omega_{\mathrm{dmd},i}$. As there is still only one output to be considered, an over-actuated system with more inputs than outputs is present. In general, feedback linearisation can also be applied to multi-input, multi-output systems (Isidori, 1995). However, it is required that the number of inputs and outputs must be equal. Such a system is called a square system. In case there exists more than one jet fan ($n_{\mathrm{JV}} > 1$), an over-actuated multi-input single-output system is present and relation (21) resulting from feedback linearisation yields

$$w^{(r)} = \mathrm{L}_f^{(r)} h(\boldsymbol{x}^*) + \sum_{i=1}^{n_{\mathrm{JV}}} \mathrm{L}_{\boldsymbol{g}_i} \mathrm{L}_f^{(r-1)} h(\boldsymbol{x}^*) \omega^*_{\mathrm{dmd},i}. \tag{26}$$

How (26) can be used to obtain the feedforward control despite n_{JV} unknown $\omega^*_{\mathrm{dmd},i}$ appearing in one equation, is shown in the next section.

4. Design of the tunnel ventilation feedforward control

To obtain a dynamic feedforward control law for the tunnel ventilation, the over-actuated system (6), which contains the dynamic relations (8) and (9), is considered. Any disturbance influences Δp_j as given in (1) are assumed to be zero. In this section two different approaches are shown to obtain the control law. The first one (Section 4.2) is focused on tracking performance, although due to the special structure of the state transformation (Section 4.3) an undesired control signal behaviour might appear. Thus, a second approach focused on robustness has been developed (Section 4.4). In addition, the reference trajectory planning and the evaluation of a feasible trajectory are shown in Section 4.5.

4.1. Controllability

An important property of the system is its current controllability. The system is controllable with input i as long as

$$\mathrm{L}_{\boldsymbol{g}_i} \mathrm{L}_f h(\boldsymbol{x}) \neq 0 \tag{27}$$

holds. Evaluating the controllability condition (27) for the tunnel ventilation (16) yields the requirements

$$2 x_{i+1} v_{\mathrm{JVmax},i} - x_1 \neq 0 \quad \text{and} \quad x_{i+1} \neq 0. \tag{28}$$

In physical terms, controllability is lost if one of the following conditions

$$\omega_i = \frac{u}{2 v_{\mathrm{JVmax},i}} \quad \text{or} \quad \omega_i = 0 \tag{29}$$

occurs. The first equation in (29) corresponds to the situation of the outlet velocity of jet fan i being equal to half the overall average air flow velocity u in the tunnel. Thus, the fanwheel is windmilling in the air flow without giving any contribution of momentum.

4.2. Performance-oriented approach

If only one jet fan is installed, the feedforward control law (25) can be used directly to feedforward control the tunnel ventilation. For the over-actuated multi-input single-output system with multiple jet fans, (26) resulting from feedback linearisation cannot be solved unambiguously without auxiliary conditions. In addition to the single equation representing the feedforward control law

$$\ddot{w} = \mathrm{L}_f^2 h(\boldsymbol{x}^*) + \sum_{i=1}^{n_{\mathrm{JV}}} \mathrm{L}_{\boldsymbol{g}_i} \mathrm{L}_f h(\boldsymbol{x}^*) \omega^*_{\mathrm{dmd},i}, \tag{30}$$

which contains n_{JV} unknown control signals $\omega^*_{\mathrm{dmd},i}$, further conditions are required. By (30) it is only determined which contribution the sum term $\sum \mathrm{L}_{\boldsymbol{g}_i} \mathrm{L}_f h(\boldsymbol{x}^*) \omega^*_{\mathrm{dmd},i}$ has to give as a whole, but not how the control action is distributed across individual jet fans.

Two possible approaches are illustrated in the following. All control signals $\omega^*_{\mathrm{dmd},i}$ are chosen equally such that (30) is fulfilled. As this choice would use all jet fans in the tunnel simultaneously, this strategy is not favourable. The priority in which the individual jet fans are to be activated is determined by the planning engineers in each tunnel individually and has to be considered in the control strategy. Thus, a simultaneous operation of all jet fans usually does not occur.

Alternatively, the jet fans are activated sequentially. Thus, only the first one is used as long as its momentum is sufficient. Subsequently, if necessary, further jet fans are included and their rotational speed is increased until (30) holds. This latter strategy is used in the performance-oriented approach.

The evaluation of the required state trajectory $\boldsymbol{x}^*$ is based on the inverse state transformation (24) and is discussed in the subsequent section.

4.3. State transformation and bifurcation

To analyse the system model (6), the tunnel with only one jet fan is considered. In return, the constraint on the rotational speed of the single jet fan is dropped such that the jet fan mathematically can also provide more than the nominal thrust. To distinguish this virtual single jet fan rotational speed from the physically feasible rotational speeds, it will be denoted by ω_{v}. The state vector

$$\boldsymbol{x} = \begin{bmatrix} x_1 \\ x_2 \end{bmatrix} = \begin{bmatrix} u \\ \omega_{\mathrm{v}} \end{bmatrix} \tag{31}$$

used for the state transformation contains the air flow velocity u in the tunnel and the virtual rotational speed ω_{v} of the single jet fan contributing the same amount of momentum as the sum of individual fans. As the resulting two-dimensional system has full relative degree, the state transformation (19) yields

$$\boldsymbol{z} = \begin{bmatrix} z_1 \\ z_2 \end{bmatrix} = \begin{bmatrix} x_1 \\ k_{\mathrm{JV,v}} v^2_{\mathrm{JVmax,v}} |x_2| \left(x_2 - \frac{x_1}{v_{\mathrm{JVmax,v}}} \right) - k_{\mathrm{Fric}} x_1 |x_1| \end{bmatrix} \tag{32}$$

and its ambiguous inverse transformation $\boldsymbol{x} = \mathcal{T}^{-1}(\boldsymbol{z})$ can be derived as

$$x_1 = z_1 \tag{33a}$$

$$x_2 = \begin{cases} \dfrac{z_1}{2 v_{\mathrm{JVmax,v}}} \pm \sqrt{\dfrac{z_1^2}{4 v^2_{\mathrm{JVmax,v}}} + c(z_1, z_2)}, & \text{if radicand } > 0 \\ \dfrac{z_1}{2 v_{\mathrm{JVmax,v}}} \mp \sqrt{\dfrac{z_1^2}{4 v^2_{\mathrm{JVmax,v}}} - c(z_1, z_2)}, & \text{otherwise} \end{cases} \tag{33b}$$

with

$$c(z_1, z_2) = \frac{z_2 + k_{\mathrm{Fric}} z_1 |z_1|}{k_{\mathrm{JV}} v^2_{\mathrm{JVmax,v}}}. \tag{34}$$

However, due to the absolute value function in (32), transformations (32) and (33) do not constitute a diffeomorphism although the system is differentially flat. Especially the inverse transformation (33b) of x_2 yields two different solutions ${}^{+}x_2^*$ and ${}^{-}x_2^*$ of which only one is physically feasible. The feasible solution can be identified by applying the transformation (32) to both solutions, where only one of them will reconstruct the original trajectory in $\boldsymbol{z}$.

By choosing the transformed state as

$$\begin{bmatrix} z_1 \\ z_2 \\ \vdots \\ z^n \end{bmatrix} = \begin{bmatrix} w \\ \dot{w} \\ \vdots \\ w^{(n-1)} \end{bmatrix}, \tag{35}$$

the required state trajectories $\boldsymbol{x}^*$ can be found from the reference

trajectory w according to (33). The choice taken in (35) is called differential parameterisation. To illustrate the state transformation, in Fig. 3 a change of operating point from flow velocity 0–1.75 m/s is shown in terms of state trajectories x_1^*, ${}^{+}x_2^*$ and ${}^{-}x_2^*$. Note that only solution ${}^{+}x_2^*$ is physically plausible as for a positive change of flow velocity, a positive rotational speed would be required. In addition, applying (25) using each of the solutions individually to obtain ${}^{+}\omega_{\mathrm{dmd}}^*$ and ${}^{-}\omega_{\mathrm{dmd}}^*$ shows that only the state ${}^{+}x_2^*$ of the feasible solution converges to its associated control signal ${}^{+}\omega_{\mathrm{dmd}}^*$ (Fig. 3). The relation of solution ${}^{-}x_2^*$ and the control signal ${}^{-}\omega_{\mathrm{dmd}}^*$ is even non-causal.

Fig. 4 shows a scenario, where the initial flow velocity at 4 m/s is higher than its reference value of 1.75 m/s. At $t = 85$ s, the two state trajectories ${}^{+}x_2^*$ and ${}^{-}x_2^*$ intersect at the abscissa. This intersection appears at the moment the controllability condition (29) is not fulfilled. As a consequence, the control signal ω_{dmd}^* obtained by the performance-oriented approach shows a singularity.

If there is more than one jet fan installed in the tunnel, the system dimension $n = n_{\mathrm{JV}} + 1$ is greater than the relative degree $r = 2$. Thus, the state transformation (19) cannot be inverted to $\boldsymbol{x}^* = \mathcal{T}^{-1}(z)$ unambiguously with differential parameterisation. In physical terms, there exists no distinct solution of jet fan rotational speed trajectories, because the required air flow trajectory could be achieved with several jet fan configurations in case of an over-actuated system. To be able to evaluate (30) nevertheless, the required state trajectories x_2^* to $x_{n_{\mathrm{JV}}+1}^*$ have been found by numerical integration of (9) instead of the inverse state transformation. For this purpose, the control signals $\omega_{\mathrm{dmd},i}^*$ are found from (30) in combination with the distribution algorithm (simultaneous or sequential operation of jet fans). Thus, in (30) $\boldsymbol{x}^*$ denotes the state vector with x_1 being replaced by the flow velocity reference w and the remaining states by the numerically integrated demand signals to complete the performance-oriented approach (Section 4.2). However, when the numerical integration is applied to a demand signal with a singularity, a bifurcation-like behaviour appears. Depending on the exact coincidence of the integration time steps with the appearance of the singularity, the demand signal can even end up on the infeasible solution branch.

As one possibility to overcome the pitfall of uncontrollability and the resulting singularity as universal as possible, a robust feedforward control will be presented in the next section. It is merely based on differential parameterisation and the state transformation rather than on any relation yielding the required input directly. By doing so, the appropriate solution branch can be selected and loss of controllability is avoided.

4.4. Robustness-oriented approach

As a safety relevant control task is considered, robustness is of uttermost importance, even though the tracking performance might decrease a little in return. To overcome the singularity issue presented in Section 4.3 and assure a flawless operation without loss of controllability, a robust approach based on the inverse state transformation (33a) is pursued by replacing the non-linear relation describing the input with an internal feedback loop to obtain the control signals $\omega_{\mathrm{dmd},i}^*$.

From the differential parameterisation (35) by using the reference air flow trajectory w and its derivative $\dot{w}$, the transformed states $\boldsymbol{z}$ are determined. Then, according to (33a), the required trajectories of the original states $\boldsymbol{x}^*$ are known, which correspond to the air flow velocity itself and the overall required thrust x_2^*.

As it was assumed in (33a) that only one jet fan without any momentum constraint exists, trajectories of the individual rotational speeds ω_i^* of the jet fans considering their maximal thrust have to be found. This is achieved by a distribution of thrust such that equivalency between the single virtual jet fan with rotational speed ω_{v}, which is contained as x_2^* in $\boldsymbol{x}^*$, and the actual thrust resulting from the sum of individual jet fans ω_i^*

$$k_{\mathrm{JV,v}} v_{\mathrm{JVmax,v}}^2 |x_2^*| x_2^* \left(1 - \frac{x_1^*}{x_2^* v_{\mathrm{JVmax,v}}}\right) = \sum_{i=1}^{n_{\mathrm{JV}}} k_{\mathrm{JV},i} v_{\mathrm{JVmax},i}^2 |\omega_i^*| \omega_i^* \left(1 - \frac{x_1^*}{\omega_i^* v_{\mathrm{JVmax},i}}\right) \tag{36}$$

holds. Thus, a thrust distribution algorithm $d(\boldsymbol{x}^*)$ shown as the first block on the left side of Fig. 5 has to ensure appropriate rotational speed trajectories ω_i^*, which fulfill (36). Thrust equivalency is achieved by fully switching on n_{on} jet fans ($\omega_i^* = \mathrm{sign}(x_2^*)$, $i = \{0, \ldots, n_{\mathrm{on}}\} \in \mathbb{N}_0$), such that the magnitude of the required rotational speed $\omega_{(n_{\mathrm{on}}+1)}^*$ ends up in the interval [0; 1]. The quadratic relation

$$|\omega_{(n_{\mathrm{on}}+1)}^*| \omega_{(n_{\mathrm{on}}+1)}^* - |\omega_{(n_{\mathrm{on}}+1)}^*| \frac{x_1^*}{v_{\mathrm{JVmax},(n_{\mathrm{on}}+1)}} - R(\boldsymbol{x}^*, n_{\mathrm{on}}) = 0 \tag{37}$$

resulting from (36) with

$$\begin{aligned} R(\boldsymbol{x}^*, n_{\mathrm{on}}) = & \frac{k_{\mathrm{JV,v}} v_{\mathrm{JVmax,v}}^2}{k_{\mathrm{JV},(n_{\mathrm{on}}+1)} v_{\mathrm{JVmax},(n_{\mathrm{on}}+1)}^2} |x_2^*| x_2^* \left(1 - \frac{x_1^*}{x_2^* v_{\mathrm{JVmax,v}}}\right) \\ & - \sum_{i=1}^{n_{\mathrm{on}}} \frac{k_{\mathrm{JV},i} v_{\mathrm{JVmax},i}}{k_{\mathrm{JV},(n_{\mathrm{on}}+1)} v_{\mathrm{JVmax},(n_{\mathrm{on}}+1)}^2} (\mathrm{sign}(x_2^*) v_{\mathrm{JVmax},i} - x_1^*) \end{aligned} \tag{38}$$

contains the unknowns $n_{\mathrm{on}} = \{0, \ldots, n_{\mathrm{JV}}\} \in \mathbb{N}_0$ and $\omega_{(n_{\mathrm{on}}+1)}^* \in [-1; 1]$. By evaluating the solution of (37), the appropriate amount n_{on} of jet fans to be switched on and the corresponding jet fan speed $\omega_{(n_{\mathrm{on}}+1)}^*$ is found under consideration of the correct sign.

Thrust control, which is equivalent to jet fan speed control, is applied separately to each jet fan i (Fig. 5) to obtain the control signals $\omega_{\mathrm{dmd},i}^*$. By using such a scheme, the control signals are ensured to be bounded. They do not show any singularities and therefore the bifurcation problem is avoided. A more aggressive thrust controller tuning results in smaller control errors and leads to tracking properties similar to the performance-oriented approach. In turn, the control signal becomes very active and usually a more moderate tuning is desirable considering a tradeoff between control signal activity and tracking performance. In this regard, also the adherence to control signal constraints, which means that $\omega_{\mathrm{dmd},i}^*$ has to remain within the interval $[-1; 1]$, has to be ensured by the individual thrust controllers.

However, applying jet fan speed controllers instead of a non-linear relation describing the input as in the performance-oriented approach introduces a delay in the actual thrust effective rotational speed ω_i. This delay will lead to an air flow velocity tracking error as compared to the original reference air flow trajectory w when the feedforward control signals $\omega_{\mathrm{dmd},i}^*$ are applied to the plant. The actually achievable trajectory u^* can directly be determined by numerical integration of (1) using the thrust effective rotational speeds ω_i (trajectory evaluation block in Fig. 5). The control signals $\omega_{\mathrm{dmd},i}^*$ and the feasible trajectory u^* represent the result of the dynamic feedforward control (compare Fig. 1). For a suitable jet fan speed controller tuning as well as a meaningfully planned air flow velocity reference trajectory w, the robust approach yields control signals $\omega_{\mathrm{dmd},i}^*$, which are more advantageous in terms of applicability to the jet fans. At the start of the control, control signals rise more slowly compared to the performance-oriented approach.

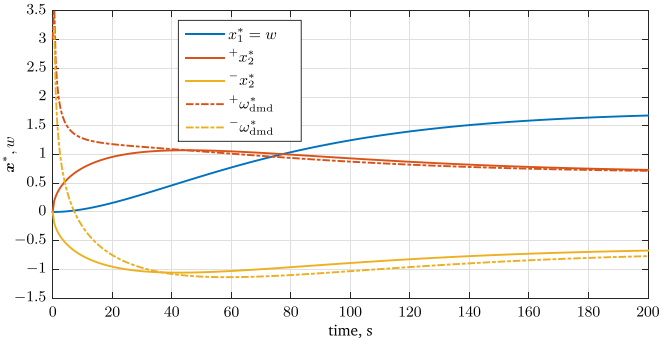

Fig. 3. Inversely transformed state trajectories for a change of flow velocity operating point from 0 to 1.75 m/s.

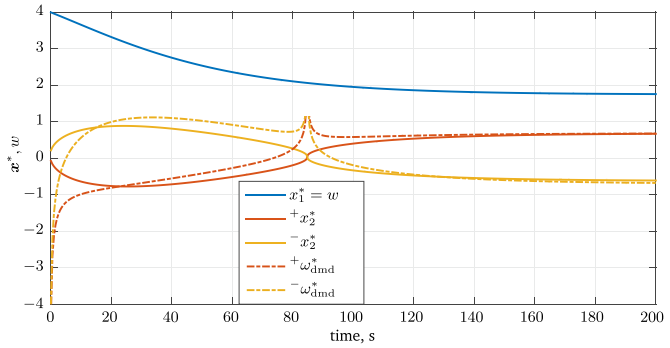

Fig. 4. Inversely transformed state trajectories for a change of flow velocity operating point from 4 m/s to 1.75 m/s.

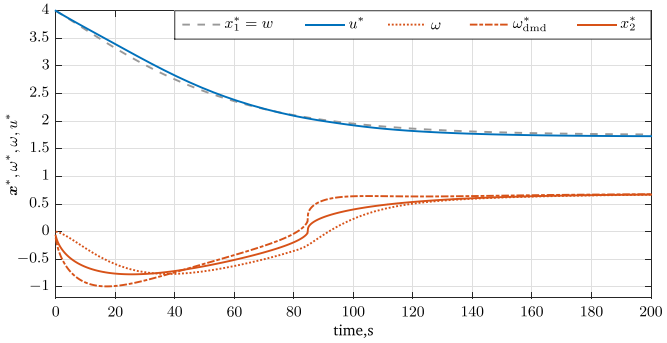

Fig. 6. Change of flow velocity operating point from 4 m/s to 1.75 m/s using the robustness-oriented approach.

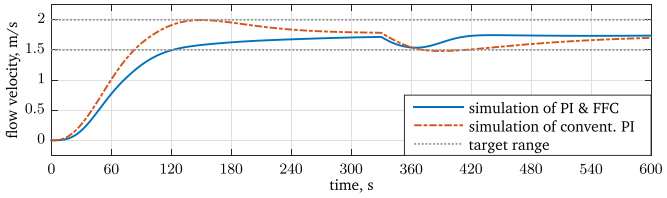

Fig. 7. Comparison of ventilation control with conventional PI control (balanced tuning, dotdashed line) and the proposed two-degrees-of-freedom control scheme (solid line); at $t = 330$ s a disturbance step acts against the direction of air flow.

In Fig. 6 the same scenario as in Fig. 4 is covered by the robustness-oriented approach. For thrust control a PI controller has been used. The control signal ω_{dmd}^* (dotdashed line) as well as the thrust-effective rotational speed ω (dotted line), which is used in the numerical integration of (1), is shown in Fig. 6.

To compare conventional feedback control of the tunnel ventilation to the proposed two-degrees-of-freedom control scheme with incorporation of the robustness-oriented feedforward control approach, simulation results are shown in Fig. 7. The emergency ventilation programme is started at $t = 0$ s. At $t = 330$ s a disturbance step acts against the direction of flow. With conventional PI control (dotdashed line) a balanced tuning considering tracking performance as well as disturbance rejection has to be applied. This requirement leads to a tuning with an overshoot in the step response. Such an overshoot is especially critical as an excessive air flow velocity can destroy the smoke stratification within the tunnel. In particular in the early stage of the emergency ventilation programme, where potentially several people are still located within the tunnel, such an overshoot represents a risk, which needs to be avoided at any cost. By using the two-degrees-of-freedom control scheme a more robust behaviour can be achieved in several aspects: The feedback part can be specifically tuned for disturbance rejection (see Fig. 7 after $t = 330$ s) as the reference tracking is achieved by the feedforward part. Although the rise time is slightly lower with the conventional controller, this fact is compensated by other considerations. To achieve short rise times, a larger number of jet fans will have to be used initially. However, they will be switched on for a short period only, which is not desirable. By applying the two-degrees-of-freedom scheme, also the control signal trajectories can be taken into account in advance. Such a consideration led to the selection of a slightly slower trajectory as it could have been achieved by using a larger number of jet fans. The rise time is not the most important performance indicator. Also the number of jet fans used, the behaviour under the influence of disturbances and especially the overshoot have to be considered in this control task.

Finally, in Section 5, application results for both feedforward control approaches are given.

4.5. Trajectory planning

The appropriate design of the reference air flow velocity trajectory w has a significant influence on the achievable tracking performance. On the one hand, the trajectory has to fulfill all control objectives such as the avoidance of overshoot or a suitable rise and settling time. On the other hand, choosing the trajectory too fast leads to inadequately active control signals, which might as well exceed the maximum thrust available. Additionally, from feedback linearisation and the relative degree it is required that the trajectory is at least two times continuously differentiable.

As an approach, which is easy to parameterise and implement, a step signal σ is filtered by a second order low-pass filter (PT2)

$$G_{\mathrm{PT2}}(s) = \frac{\omega_n^2}{s^2 + 2\zeta\omega_n s + \omega_n^2} \tag{39}$$

to yield the required trajectory w. The parameters of the PT2 are the damping ratio ζ as well as the undamped natural angular frequency ω_n. By choosing the aperiodic boundary case ($\zeta = 1$), overshoot is avoided and the characteristic values in the time domain are determined solely by ω_n.

Expressing the PT2 filter as a state space system

$$\begin{bmatrix} \dot{w} \\ \ddot{w} \end{bmatrix} = \begin{bmatrix} 0 & 1 \\ -\omega_n^2 & -2\zeta\omega_n \end{bmatrix} \begin{bmatrix} w \\ \dot{w} \end{bmatrix} + \begin{bmatrix} 0 \\ \omega_n^2 \end{bmatrix} \sigma, \tag{40}$$

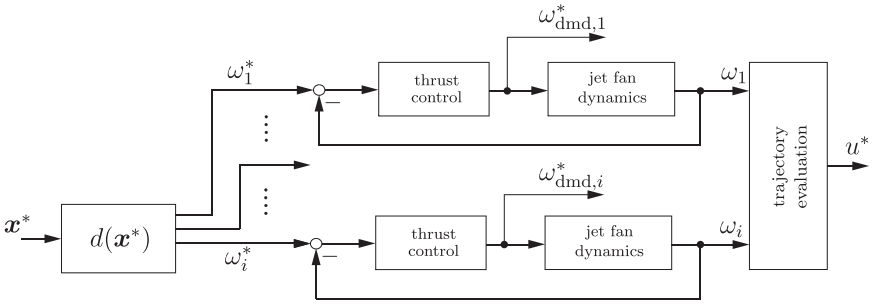

Fig. 5. Block diagram of the robustness-oriented approach with the thrust equivalency distribution $d(\boldsymbol{x}^*)$ of the required momentum to the individual jet fan trajectories ω_i^* and control loops to obtain the control signals $\omega_{\mathrm{dmd},i}^*$ as well as current thrust-effective rotational speeds ω_i.

provides the opportunity not only to prescribe the initial value w_0 of the trajectory to the current air flow velocity, but also to set the initial gradient $\dot{w}_0$ at the start of control to values different from zero. The initialisation of the gradient can be used to ensure, that the trajectory x_2^* of the desired rotational speed starts at zero, which is achieved by setting

$$\dot{w}_0 = -k_{\mathrm{Fric}} w_0 |w_0|. \tag{41}$$

When the emergency ventilation programme starts, the current air flow velocity is used as the initial value w_0 of the reference. By choosing (41) as the initial gradient, the system is initialised in a naturally plausible state. More important, it is ensured that x_2^* starts at zero and no adverse activation of jet fans occurs after the start of control. This way of initialisation has already been used in the simulations in Figs. 3 and 4.

Ideally, the choice of the optimal natural angular frequency ω_n as the single parameter of trajectory generation is made with consideration of the initial conditions. In particular, the required settling time, the initial deviation of the current from the reference air flow velocity, as well as the maximum number of jet fans used during the operating point change, should be considered when choosing ω_n.

The reference air flow velocity trajectory w obtained by (40) serves as reference for the feedforward control, whereas the reference u_{m}^* for the feedback controller usually is different (see Fig. 1). The latter signal represents that physically feasible trajectory, which will be observed at the measurement device when applying the feedforward control to the plant without correcting feedback control. Even in case the feedforward control could achieve perfect tracking of w, the measurement dynamics Σ_{m} would still cause a control error arising only from its low-pass behaviour. First, u^* is the result of the feedforward control considering the actual thrust-effective rotational speed signals ω_i (see Fig. 5). The resulting actual air flow velocity u^* is used as input into the measurement dynamics (5) to obtain u_{m}^*.

5. Results

The proposed non-linear dynamic feedforward control has been implemented and tested in winter/spring 2015/2016 in the southern tube of the St. Ruprecht motorway tunnel on the Austrian Semmering motorway S6 in course of an encompassing tunnel refurbishment and modernisation. Thus, experiments could have been carried out while the tunnel was closed to traffic. During the final commissioning also a test with an actual fire has been conducted.

The control objectives of the tunnel ventilation are defined by the Austrian standard RVS (2014). It is required, that in case of an emergency, the fire programme automatically starts after the detection of a fire. In one-directional tunnel operation the target range of the air flow velocity is 1.5 m/s to 2 m/s; in bi-directional operation 1.0 m/s to 1.5 m/s. The direction of the air flow has to coincide with the direction of traffic, except for bi-directional operation, where the current air flow direction at ventilation start has to be maintained. In both cases, the air flow velocity target range has to be reached and kept after 300 s at most (settling time). The sequential priority in which the individual jet fans are to be activated is determined by the planning engineers in each tunnel individually, usually starting with those located downstream of the fire location. Jet fans located within the affected fire area are excluded and must not be used for ventilation.

5.1. Description of plant

The considered southern tube of the one-directional motorway tunnel St. Ruprecht is located on the Austrian Semmering motorway S6 southwest of Bruck an der Mur in Styria. It is 619 m long, has a slight uphill gradient of 1.3% and runs in a left turn in direction of travel. A schematic drawing of the considered tube and its installations is shown in Fig. 8. Three jet fans are installed along the tunnel. Except of that

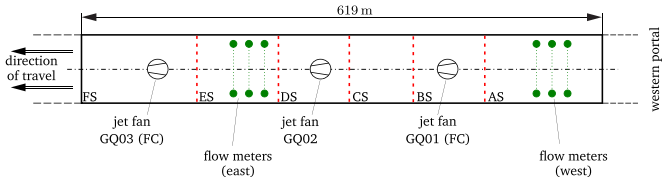

Fig. 8. Schematic layout and installation scheme of the southern tube of motorway tunnel St. Ruprecht on Semmering motorway S6.

one in the centre of the tunnel, the other two jet fans are equipped with frequency converters (FC). In case of a fire detection, that jet fan located nearest to the triggering fire area (denoted AS to FS in Fig. 8) remains switched off permanently. Thus, at least one jet fan with FC remains available and a continuous control signal can be deployed. The longitudinal flow velocity is measured by two independent measurement locations consisting of three measurement devices each. Depending on the fire location, the average value of the three values of one of the measurement cross sections east or west is used for control. In standard operation, fire detection is achieved by heat detectors located at the tunnel ceiling or alternatively also by smoke detection by means of image processing of video surveillance cameras. When experiments are conducted, the emergency programme is triggered manually in one of the fire areas.

5.2. Model parameterisation from data

The non-linear model of the tunnel air flow (Section 2) has been derived from physical considerations and is valid for different tunnels likewise. Solely choosing the model parameters adequately, ultimately determines the model accuracy for a particular tunnel. Usually, the parameters are either known exactly, e. g. the tunnel dimensions, or they are determined from expert knowledge. Although a proper model results from these base parameters already, the model accuracy can be further improved by data-based modelling (Ljung, 1999).

To obtain optimised parameters, open-loop experiments have to be conducted first. For this purpose, an excitation signal is applied to the plant, which is used together with the measured output and the model equations in a subsequent parameter optimisation. How such an excitation signal can be chosen to excite the system and its non-linearity in an optimal way, is answered by design of experiment techniques (Nelles, 2001). In the application to the tunnel, an amplitude modulated pseudo-random binary sequence (APRBS) with variable hold times has been used. In the lower panel of Fig. 9, the applied signals of the individual jet fans are depicted. Jet fan GQ02 (dashed line) located in the middle of the tunnel is not equipped with a frequency converter, thus it is switched on and off only. In the upper panel, the individual air flow velocity measurements of the western measurement cross section are shown as dashed lines. Their mean value $u_{\mathrm{m,west}}$ is given as solid line. Due to the curved tunnel axis, jet fan GQ02 has a disturbing effect on the flow measurements, which is more evident in the eastern measurements located directly downstream of jet fan GQ02. Nevertheless, the segment in time when the relevant jet fan is in operation has been excluded from the parameter optimisation using the western values. In the upper panel of Fig. 9, the average air flow velocity measurement in the excluded interval (175 s to 940 s) is characterised by a dashed line instead of the solid line.

For the parameter optimisation, the output error method (Ljung, 1999) is applied. In this approach, the difference between the dynamically simulated air flow velocity using the non-linear model and the measured air flow velocity is minimised by changing the parameters of the simulation model. Starting from an expert knowledge parameterisation $\boldsymbol{\theta}_0 \in \mathbb{R}^p$, an additive variation $\Delta\boldsymbol{\theta} \in \mathbb{R}^p$ is found to correct the parameters accordingly. If the initial parameterisation $\boldsymbol{\theta}_0$ were correct, the additive variation would remain zero. Thus, in the optimisation a regularisation term with a non-negative definite diagonal weighting matrix $\boldsymbol{R} \in \mathbb{R}^{p\times p}$ is

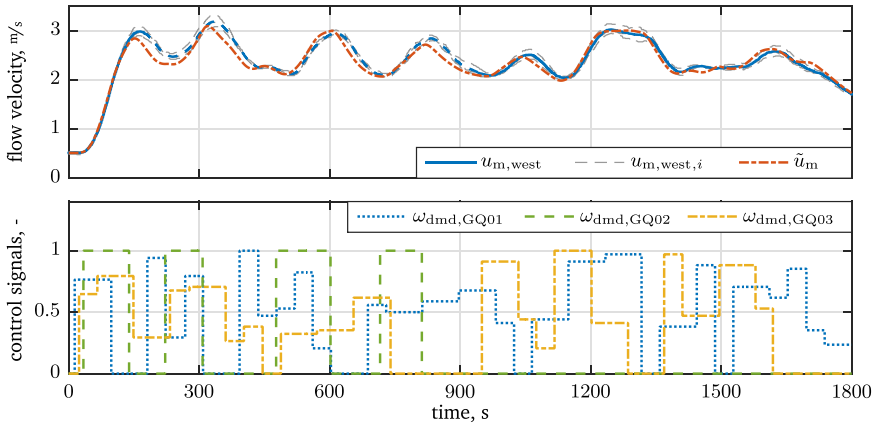

Fig. 9. Open-loop experiment for model identification and a simulation result, Upper Panel: mean (solid line) and individual measurements (dashed line) of air flow velocity as well as the simulated model output $\tilde{u}_{\mathrm{m}}$ (dotdashed line), Lower Panel: jet fan control signals applied to the plant and the simulation model.

included to penalise strong deviations from $\boldsymbol{\theta}_0$, assuming the expert knowledge to be approximately correct. Finally, the optimal parameters $\boldsymbol{\Delta\theta}$ minimize the quadratic criterion

$$\mathcal{L} = \boldsymbol{e}^{\mathrm{T}}\boldsymbol{\Psi}\boldsymbol{e} + \boldsymbol{\Delta\theta}^{\mathrm{T}}\boldsymbol{R}\boldsymbol{\Delta\theta}, \tag{42}$$

where $\boldsymbol{e} \in \mathbb{R}^{n_{\mathrm{S}}}$ contains the model error (difference between simulation and measurement) at each of the n_{S} sampling instants. The positive semi-definite diagonal matrix $\boldsymbol{\Psi} \in \mathbb{R}^{n_{\mathrm{S}} \times n_{\mathrm{S}}}$ is used to exclude the interval 175 s to 940 s from the cost function (42) and has no influence otherwise. However, it could also be used to weight different segments differently. The optimisation of (42) is done numerically using the Quasi-Newton method (Nocedal & Wright, 2006).

In the application of the output error method, not all available parameters of the air flow model should be used. The impact of individual parameters on the same effect such as for example the thrust, can not be distinguished. Additionally, the complexity of the optimisation is reduced. Only the following key parameters have been included into the optimisation, each influencing a different effect in the model: the friction coefficient λ, the installation correction factor k_{e} of the jet fans (contained in k_{JV}, thus determining the thrust of a jet fan) and the time constant τ_{JV} of the dynamic behaviour of the jet fans. The optimisation result of these parameters is shown in the lower part of Table 1. Additionally, also the pressure difference Δp is considered as a parameter, which is assumed to remain constant over the whole optimisation interval. In the upper panel of Fig. 9 the simulated air flow velocity using the optimised parameters given in Table 1 and a constant pressure difference of 473 mPa is shown as dotdashed line. The deviation of the simulation from the mean measurement (solid line) and the deviation of the individual measurements from the mean measurement is comparable. A model, which deviates from the mean velocity less than the individual measurements would not be reasonable and should even be considered as overfit. Hence, the model fit using the optimised parameters is good. Similar model fits as shown in Fig. 9 are achieved in several cross-validation simulations. However, the constant pressure difference Δp as a disturbance influence has to be adjusted in the simulations individually to match that of the considered dataset.

5.3. Experiments in the tunnel

The presented dynamic model-based feedforward control using the identified parameters from Section 5.2 has been implemented in a two-degrees-of-freedom control scheme as described previously. With this control scheme, experiments in the empty tunnel without an actual fire have been carried out first. As part of the final commissioning, finally also a test with an actual fire has been conducted.

A standard linear PI controller has been used as feedback controller in the two-degrees-of-freedom control scheme for disturbance rejection. Its tuning has been carried out using an operating point linearisation of the non-linear plant in combination with linear design methodologies. In particular, a phase margin of 53 degrees has been used as design target. The resulting controller transfer function is

$$G_{\mathrm{PI,FB}}(s) = 0.7012 + 6.6{\cdot}10^{-3}\frac{1}{s}. \tag{43}$$

In the robustness-oriented approach, also the tuning of the jet fan speed controllers (Fig. 5) has to be performed. Controller parameters have been obtained by prescribing a desired closed-loop rise time of 36 s and a maximum overshoot of 6%. The jet fan speed controller used in the following experiments is

$$G_{\mathrm{PI,JV}}(s) = 1.5 + 0.1198\frac{1}{s}. \tag{44}$$

By means of this tuning, a more or less aggressive behaviour of the feedforward control can be achieved.

All experiments basically represent an operating point change from the current air flow velocity at the start of the emergency programme to the desired value, which is chosen as the mean value between upper and lower target range bound. For comparison, in Fig. 10 a test run using the performance-oriented approach starting at an air flow velocity close to zero is shown. The zero point on the time scale is set to the instance of the manual triggering of the emergency programme. In the upper panel the reference trajectory with $\omega_n = 0.025$ 1/s is shown as solid line and the measured air flow velocity using the western flow meters (Fig. 8) as dotdashed line. The target range bounds of 1.5 m/s and 2 m/s are given as dotted lines. In the lower panel the control signals are depicted. The sum of jet fan feedforward control signals $\omega^*_{\mathrm{dmd},i}$ is shown as solid line. The contribution of feedback control is superimposed and depicted as the sum of $\omega_{\mathrm{dmd},i}$ as solid line such that the feedback correcting influence can be visualized by the grey area. Additionally, in the lower panel also the individual control signals $\omega_{\mathrm{dmd},i}$ applied to the jet fans are given. Altogether the tracking result is satisfactory and the target range is reached in 120 s, which is less than half the required time of 300 s. The dynamic feedforward control works excellently as necessary feedback corrections are minimal.

Table 1
Upper table: predefined model parameters, Lower table: optimised model parameters.

L	619 m	ρ	1.15 kgm^{-3}
D_{hydr}	7.6 m	A_{Tunnel}	52.5 m^2
v_{JVmax}	27.4 m/s	τ_{m}	3 s
τ_{JV}	22 s	k_{JV}	2.9018·10^{-5} m^{-1}
k_{Fric}	2.5·10^{-3} m^{-1}		

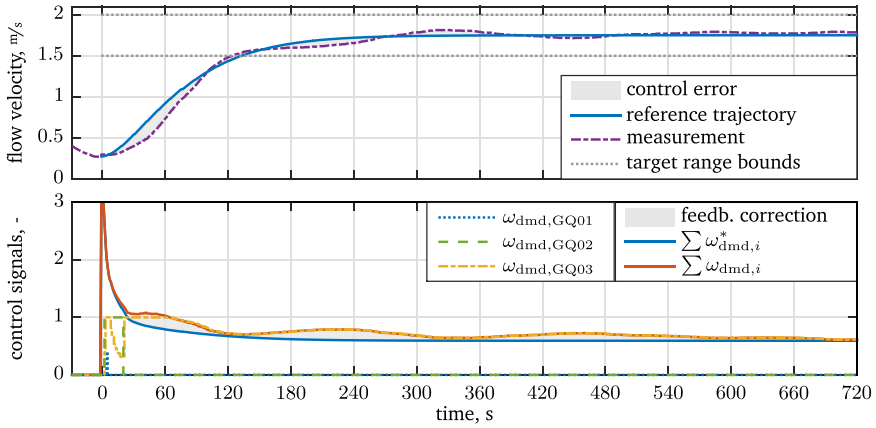

Fig. 10. Two-degrees-of-freedom controlled experiment (performance-oriented approach), Upper Panel: reference trajectory (solid line) and measurement (dotdashed line) of air flow velocity, Lower Panel: sum of jet fan feedforward control signals $\sum \omega^*_{\mathrm{dmd},i}$ (solid blue line) and together with the feedback correction $\sum \omega_{\mathrm{dmd},i}$ (solid red line) as well as the individual control signals applied to the jet fans.

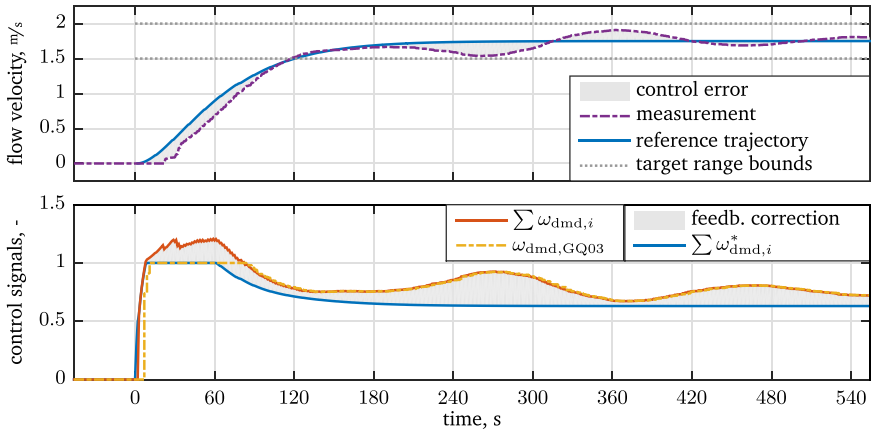

Fig. 11. Two-degrees-of-freedom controlled experiment (robustness-oriented approach), Upper Panel: reference trajectory (solid line) and measurement (dotdashed line) of air flow velocity, Lower Panel: sum of jet fan feedforward control signals $\sum \omega^*_{\mathrm{dmd},i}$ (solid blue line) and together with the feedback correction $\sum \omega_{\mathrm{dmd},i}$ (solid red line) as well as the actual control signal applied to the jet fan.

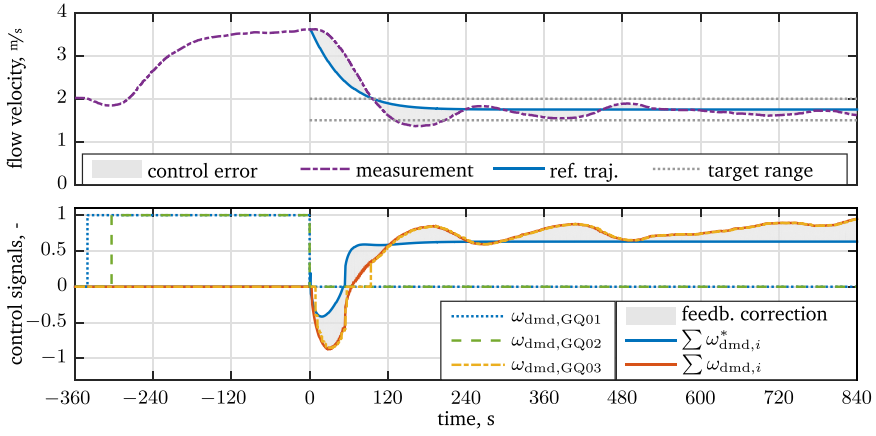

Fig. 12. Two-degrees-of-freedom controlled experiment (robustness-oriented approach) starting from above the velocity target range, Upper Panel: reference trajectory (solid line) and measurement (dotdashed line) of air flow velocity, Lower Panel: sum of jet fan feedforward control signals $\sum \omega^*_{\mathrm{dmd},i}$ (solid blue line) and together with the feedback correction $\sum \omega_{\mathrm{dmd},i}$ (solid red line) as well as the actual control signals applied to the jet fans. (For interpretation of the references to color in this figure legend, the reader is referred to the web version of this article.)

Apart from the controllability and bifurcation issues (see Section 4.3), the initial behaviour of the control signals associated with the performance-oriented approach is not favourable for application to the jet fans (Fig. 10, lower panel). The momentum peak demand at the beginning of the ventilation control leads to the activation of a large number of jet fans simultaneously and for a short time only, which can lead to electrical overload. This issue could be addressed by an elaborate trajectory adaptation considering the control signal behaviour. However, by using the robustness-oriented approach, adequate control signals are obtained. In Fig. 11 a test run with similar starting

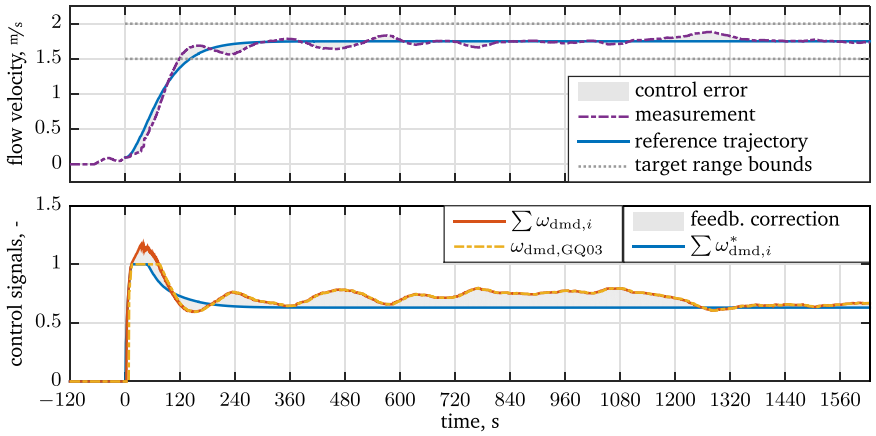

Fig. 13. Two-degrees-of-freedom controlled fire experiment (robustness-oriented approach), Upper Panel: reference trajectory (solid line) and measurement (dotdashed line) of air flow velocity, Lower Panel: sum of jet fan feedforward control signals $\sum \omega^*_{\mathrm{dmd},i}$ (solid blue line) and together with the feedback correction $\sum \omega_{\mathrm{dmd},i}$ (solid red line) as well as the actual control signal applied to the jet fan. (For interpretation of the references to color in this figure legend, the reader is referred to the web version of this article.)

conditions to the previous one is shown using the robustness-oriented approach instead. The illustration of signals is equivalent to Fig. 10. Although a slightly faster reference trajectory is used ($\omega_n = 0.03\ \mathrm{s}^{-1}$), only one jet fan becomes active. During the first 80 s of the ventilation control, the required two-degrees-of-freedom control signal is not fully applied to the jet fans as no second jet fan becomes active. The reason for this behaviour lies in the underlying frequency converter control, which does not allow rotational speeds below 30%. However, with such a low rotational speed the momentum contribution of a jet fan is nearly negligible. Thus, the trajectory tracking performance is nevertheless good.

In Fig. 12 the emergency ventilation has been triggered at a high initial air flow velocity of 3.6 m/s. To reach this condition, two jet fans (dotted line and dashed line in the lower panel of Fig. 12) have been activated manually for 350 s ahead of the start of control at point in time 0 s. The feedforward control signal (solid line in the lower panel) initially acts against the direction of flow to decelerate the air flow and finally returns to positive values to maintain the steady state. Feedback control overcompensates during the first 60 s, which leads to a slight undershoot at point in time 170 s. This overcompensation is caused by the non-stationary initialisation of the reference trajectory ($\omega_n = 0.03\ \mathrm{s}^{-1}$), which assumes the gradient to be given as in (41). However, due to the inertia of the air in the tunnel the velocity remains constant after switching off jet fans GQ01 and GQ02. The resulting control error entails the overcompensation and the slight undershoot. Such a behaviour could have been avoided by waiting a small amount of time between switching off the manually controlled jet fans and triggering the emergency ventilation. Despite the undershoot, the target range is reached and kept after 200 s.

Finally, a test with an actual fire in the tunnel has been conducted. Two steel trays with an area of 1 m^2 each filled with 25 l of a mixture of fuel and diesel have been used as fire source. The trays have been located at the boundary between fire sections CS and DS and the fire has been detected automatically in less than a minute after ignition in section DS. In Fig. 13 the result of the fire test is depicted. The air flow velocity reaches the target range in less than 120 s after the fire detection. The reference trajectory ($\omega_n = 0.025\ \mathrm{s}^{-1}$) is followed with slight deviations only and feedback control action is minimal. Thus, the model used in the dynamic feedforward control robustly applies also when a fire is present.

Note that in the control signal (Fig. 13, lower panel) a slight disturbance influence is visible. In the time interval 800 s to 1100 s, the air flow velocity remains constant at 1.75 m/s with a rotational speed of approximately 75%. From 1320 s onwards, exactly the same air flow velocity is achieved, but with significantly less rotational speed of only 63%. The latter value exactly matches with the feedforward control signal. Thus, a disturbance influence, which changed in between these intervals, is obviously present.

6. Conclusion & outlook

In this paper, an approach to obtain a model-based dynamic feedforward control as a non-linear extension of common linear feedback control has been presented for the longitudinal ventilation of road tunnels in case of an emergency with fire and smoke. For this purpose, feedback linearisation has been applied to the non-linear model of the air flow in the tunnel. The associated transformations and equations have been shown and analysed, and finally a robust approach has been tested and implemented. In several experiments without and with an actual fire, the practical applicability and performance of the feedforward control has been demonstrated.

When new jet fans are installed in tunnels, they are usually equipped with frequency converters. However, in existing installations mostly a switching fan operation can be used only. Additionally, a jet fan has to remain switched on for a minimum period of time as soon as it has been started. A similar restriction applies when switching it off. In future work, a feedforward algorithm could focus especially on such an actuator setup.

In either case, efficient disturbance rejection is a crucial part of a successful control scheme. In the second paper on tunnel ventilation (Fuhrmann et al., 2017) a non-linear disturbance observer (pressure drop observer) with special structure is proposed and tested in the tunnel. The estimated pressure drop is used for disturbance rejection and basically renders the feedback controller redundant, thus significantly improving control performance. The applicability is also shown in experiments in the tunnel.

References

Bendelius, A. G., (1996). *Tunnel Engineering Handbook*, 2nd Edition. Kluwer Academic Publishers, Boston/Dordrecht/London, Ch. Tunnel Ventilation, pp. 384–438.

Bogdan, S., Birgmajer, B., & Kovacić, Z. (2008). Model predictive and fuzzy control of a road tunnel ventilation system. *Transportation Research Part C, 16*, 574–592.

Chen, P.-H., Lai, J.-H., & Lin, C.-T. (1998). Application of fuzzy control to a road tunnel ventilation system. *Fuzzy Sets and Systems, 100*, 9–28.

Chu, B., Kim, D., Hong, D., Park, J., Chung, J., Chung, J.-H., & Kim, T.-H. (2008). GA-based fuzzy controller design for tunnel ventilation systems. *Automation in Construction, 17*, 130–136.

Cory, W. T. W. (2005). *Fans & ventilation: a practical guide*. Elsevier.

Danzer, M. A., Wilhelm, J., Aschemann, H., & Hofer, E. P. (2008). Model-based control of cathode pressure and oxygen excess ratio of a PEM fuel cell system. *Journal of Power Sources, 176(February (2))*, 515–522.

Ferkl, L., & Meinsma, G. (2007). Finding optimal ventilation control for highway tunnels. *Tunnelling and Underground Space Technology, 22*, 222–229.

Fliess, M., Lévine, J., Martin, P., & Rouchon, P. (1995). Flatness and defect of non-linear systems: introductory theory and examples. *International Journal of Control, 61*,

1327–1361.
Fuhrmann, M., Euler-Rolle, N., Killian, M., Reinwald, M., & Jakubek, S., (2016). Longitudinal tunnel ventilation control. *Part 2: Non-linear observation and disturbance rejection*. Control Engineering Practice, doi: 10.1016/j.conengprac.2017.03.016, (in this issue).
Hagenmeyer, V., & Delaleau, E. (2003). Exact feedforward linearization based on differential flatness. *International Journal of Control, 76(6)*, 537–556.
Horn, J., Bamberger, J., Michau, P., & Pindl, S. (2003). Flatness-based clutch control for automated manual transmissions. *Control Engineering Practice, 11(12)*, 1353–1359.
Horowitz, I. M. (1963). *Synthesis of feedback systems* New York: Academic Press.
Hrbcek, J., Spalek, J., & Šimák, V., January 28–30 (2010). Process Model and Implementation the Multivariable Model Predictive Control to Ventilation System. In: *Proceedings of the 8th IEEE International Symposium on Applied Machine Intelligence and Informatics*. Herl'any, Slovakia, pp. 211–214.
Isidori, A., (1995). Nonlinear Control Systems, 3rd Edition. *Communications and Control Engineering*. Springer-Verlag London.
Karakas, E. (2003). The control of highway tunnel ventilation using fuzzy logic. *Engineering Applications of Artificial Intelligence, 16*, 717–721.
Khalil, H. K. (2002). *Nonlinear systems* (3rd ed.) Upper Saddle River: Prentice Hall.
Kurka, L., Ferkl, L. O., & Porízek, J., Jul. (2005). Simulation of traffic, ventilation and exhaust in a complex road tunnel. In: *16th IFAC World Congress*. Prague, Czech Republic, pp. 60–65.
Ljung, L., (1999). System Identification: Theory for the User, 2nd Edition. *Prentice Hall Information and System Sciences Series*. Prentice Hall PTR, Upper Saddle River.
Malchow, F., & Sawodny, O. (2012). Model based feedforward control of an industrial glass feeder. *Control Engineering Practice, 20(1)*, 62–68.
Nakahori, I., Mitani, A., & Vardy, A., 3.–4. May (2010). Automatic control of two-way tunnels with simple longitudinal ventilation. In: *Proceedings of the 5th International Conference on Tunnel Safety and Ventilation*. Graz, Austria, pp. 74–84.
Nelles, O., (2001). *Nonlinear System Identification*. Vol. 13 of Measurement Science and Technology. Springer, Berlin/Heidelberg.
Nocedal, J., & Wright, S. J., (2006). *Numerical Optimization*, 2nd Edition. Springer Series in Operation Research and Financial Engineering. Springer Science + Business Media, New York.
PIARC, (2011). Road Tunnels: Operational Strategies for Emergency Ventilation. Tech. rep., *World Road Association (PIARC)*, Technical Committee 3.3 Road Tunnel Operation, La Defense cedex, France.
RVS 09.02.31, Jun. (2014). *Tunnel Ventilation - Basic Principles*, Austrian Research Association for Roads, Railways and Transport, Wien.
Slotine, J.-J. E., & Li, W. (1991). *Applied nonlinear control* Englewood Cliffs: Prentice Hall.
Sturm, P., Bacher, M., Schmölzer, G., & Beyer, M., 3.–4. May (2010). Ventilation design tools and validation. In: *Proceedings of the 5th International Conference on Tunnel Safety and Ventilation*. Graz, Austria, pp. 173–180.
Sturm, P., Beyer, M., & Rafiei, M., (2015). On the problem of ventilation control in case of a tunnel fire event. *Case Studies in Fire Safety* [in press], http://dx.doi.org/10.1016/j.csfs.2015.11.001.
Tan, Z., Huang, Z., Wu, K., & Xu, L., 16.–19. Sept (2012). Simulation analysis of longitudinal ventilation system with jet fan speed control for MPC strategy in a road tunnel. In: *Proceedings of the 15th International IEEE Conference on Intelligent Transportation Systems*. Anchorage, Alaska, pp. 1471–1476.